

Open Access Article

Enhanced Surface Wind Stress over the Sangihe-Talaud Islands Waters during the Extreme Climate Events of 2015 and 2019

Riza Yuliratno Setiawan^{1*}, Lilik Maslukah², Nurjannah Nurdin³, Anindya Wirasatriya², Eko Siswanto⁴, Benny Hartanto⁵

¹ Department of Fisheries, Faculty of Agriculture, Universitas Gadjah Mada, Yogyakarta, Indonesia

² Department of Oceanography, Faculty of Fisheries and Marine Science, Diponegoro University, Semarang, Indonesia

³ Department of Marine Science, Faculty of Marine Science and Fisheries, Hasanuddin University, Makassar, Indonesia

⁴ Earth Surface System Research Center (ESS), Research Institute for Global Change (RIGC), Japan Agency for Marine-Earth Science and Technology (JAMSTEC), Yokohama, Japan

⁵ Yogyakarta Maritime College (STIMARYO), Yogyakarta, Indonesia

Abstract: The ocean region off the Sangihe-Talaud Islands (STI) is pivotal because it provides a pathway for the Indonesian Throughflow and is situated in the epicenter of global marine biodiversity. However, until today sea surface variability of the region is poorly studied due to lacked long-term in situ measurements. The present research aims to elucidate the seasonal and interannual variability of surface winds and the effect of 2015 El Niño-Southern Oscillation (ENSO) and 2019 Indian Ocean Dipole (IOD) on the ocean surface off the STI by analyzing long-term datasets (2007-2019) of satellite-derived sea surface wind, sea surface temperature (SST), and surface chlorophyll-a concentration. The present research serves as the first investigation on the mesoscale atmosphere-ocean interaction in the region. It aims to provide a better understanding of the sea surface dynamics of the STI. Results show that the prevailing northeasterly and southerly winds over the STI waters induce SST cooling and phytoplankton bloom. Furthermore, our correlation analysis revealed that the ENSO plays a dominant role in affecting sea surface conditions off the STI than the IOD, presumably due to its proximity to the Pacific Ocean. This inference is also supported by anomaly analysis that shows robust effects during the climate extreme events of 2015 compared to 2019. Collectively, the results of this research highlight the importance of extreme climate events in shaping ocean conditions.

Keywords: wind, chlorophyll-a, El Niño-Southern Oscillation, Indian Ocean Dipole, Sangihe-Talaud Islands.

2015 年和 2019 年極端氣候事件期間桑吉赫-塔勞群島水域的地表風應力增強

摘要：桑吉赫-塔勞群島附近的海洋區域至關重要，因為它為印度尼西亞通流提供了一條通道，並且位於全球海洋生物多樣性的中心。然而，直到今天，由於缺乏長期的原位測量，對該地區海面變化的研究很少。本研究旨在通過分析長期數據集（2007 -2019）衛星衍生的海面風、海面溫度和地表葉綠素-a 濃度。本研究是對該地區中尺度大氣-海洋相互作用的首次調查。它旨在更好地了解桑吉赫-塔勞群島的海面動力學。結果表明，桑吉赫-塔勞群島水域盛行的東北風和南風導致海面溫度冷卻和浮游植物大量繁殖。此外，我們的相關分析表明，

Received: June 16, 2021 / Revised: August 12, 2021 / Accepted: September 18, 2021 / Published: October 30, 2021

Fund Project: Universitas Gadjah Mada PPKI Research Grant 2020 (1519/UN1/DITLIT/DIT-LIT/PT/2020)

About the authors: Riza Yuliratno Setiawan, Department of Fisheries, Faculty of Agriculture, Universitas Gadjah Mada, Yogyakarta, Indonesia; Lilik Maslukah, Department of Oceanography, Faculty of Fisheries and Marine Science, Diponegoro University, Semarang, Indonesia; Nurjannah Nurdin, Department of Marine Science, Faculty of Marine Science and Fisheries, Hasanuddin University, Makassar, Indonesia; Anindya Wirasatriya, Department of Oceanography, Faculty of Fisheries and Marine Science, Diponegoro University, Semarang, Indonesia; Eko Siswanto, Earth Surface System Research Center (ESS), Research Institute for Global Change (RIGC), Japan Agency for Marine-Earth Science and Technology (JAMSTEC), Yokohama, Japan; Benny Hartanto, Yogyakarta Maritime College (STIMARYO), Yogyakarta, Indonesia

Corresponding author Riza Yuliratno Setiawan, riza.y.setiawan@ugm.ac.id

厄爾尼諾-南方濤動在影響桑吉赫-塔勞群島以外的海麵條件方面比印度洋偶極子起主導作用，這可能是因為它靠近太平洋。這一推論也得到了異常分析的支持，該分析顯示與 2019 年相比，2015 年的氣候極端事件產生了強勁的影響。總的來說，這項研究的結果突出了極端氣候事件在塑造海洋條件方面的重要性。

关键词：風、葉綠素-一種、厄爾尼諾-南方濤動、印度洋偶極子、桑吉赫-塔勞群島。

1. Introduction

Sea surface winds play a pivotal role in regulating ocean surface conditions in the Indonesian Seas. Typically, the northwesterly (southeasterly) winds exert downwelling (upwelling) in many coastal areas in the Indonesian Seas, as indicated by high (low) sea surface temperature (SST) [1-3]. Variability of the wind is principally influenced by the Australian Indonesian Monsoon (AIM) system, which generates the prevailing of northwesterly winds during Northwest Monsoon (from December to March) and the southeasterly winds during Southeast Monsoon (from June to September) [4]. The northwesterly winds blow from the Eurasian continent, bring warm and moist air to Indonesia, and cause heavy rainfall over the region. The southeasterly winds blow from the Australian continent, carry warm and dry air to Indonesia, and induce a dry season [4]. Furthermore, sea surface condition of the Indonesian Seas is also modulated by the El Niño-Southern Oscillation (ENSO) and the Indian Ocean Dipole (IOD), i.e., the sea surface experiences strong wind forcing during El Niño/positive IOD year and weak wind forcing during La Niña/negative IOD year [1], [5-7]. Hence, examining the variability of the AIM winds and their effect on the sea surface is essential for the Indonesian fisheries management areas' marine and coastal resource management.

The Sangihe and Talaud Islands (henceforth STI) are situated in northeastern Indonesia and comprise 105 islands [8]. The Ocean region off the STI serves as a fishing hotspot for commercial fishes [8]. The STI waters are characterized by complex bathymetry. They are connected to the Pacific Ocean in the east, the Sulawesi Sea in the west, the Philippines waters in the north, and the Maluku Sea in the south (Fig. 1). Moreover, the ocean region off the STI is crucial because it provides a pathway for water mass transport from the Pacific Ocean to the Indian Ocean, known as the Indonesian Throughflow [9]. Also, it is located in the heart of the Coral Triangle, one of the most diverse sites due to its high species richness of plankton coral, demersal fish, and sea turtle [10-11]. From a socio-economic perspective, this biodiverse region provides food resources and tourism services for the people who live in its coastal areas. So far, the importance of

coastal and marine resources off the STI has been well defined. However, physical forcing like monsoon wind that controls oceanographic conditions off the STI is poorly constrained due to a lack of long-term *in situ* measurement. This wind may have played a substantial role in sustaining the life of the marine realm in the region.

The ENSO is interannual climate variability occurred in the tropical Pacific Ocean [12]. Meanwhile, the IOD is a climate mode associated with zonal SST gradient (east-west) in the Indian Ocean [13]. The El Niño event of 2015/2016 has been suggested as one of the robust El Niño events in history [14-15]. It was characterized by large positive SST anomalies that dominated the tropical Pacific Ocean basin [16]. Reference [17] suggested the multiple westerly wind bursts were liable for the water mass advection from the western Pacific warm pool into the central Pacific, which enhanced the development of a strong El Niño like in 2015. Another recent extreme event that is fascinating to be studied is the extreme positive IOD event that occurred during boreal fall 2019. The primary forcing of the 2019 positive IOD event was thought to be enhanced sea level pressure over Australia and declined sea level pressure over the South China Sea since May 2019 [18]. This inter-hemispheric sea level pressure gradient invoked the northward cross-equator over the Indonesian Seas. It accelerated wind speed over the southeastern tropical Indian Ocean, leading to the evolution of positive IOD events via Kelvin waves forcing [18, 19]. We believe the two extreme climate events of 2015 and 2019 have profound effects on the oceanic condition of the Indonesian Seas. Given the importance of the ocean region off the STI, disentangling the detailed effect of both climate events on the surface wind and sea surface condition will contribute to the successful prediction of future climate extreme events in the region. Herein, we analyze 12 years (2007-2019) of satellite-derived sea surface wind, SST, and chlorophyll-a data to understand the effects of the 2015 El Niño and the 2019 positive IOD events on sea surface wind variability over the STI waters. Results of this research can be used for better managing marine and fisheries resources in the STI.

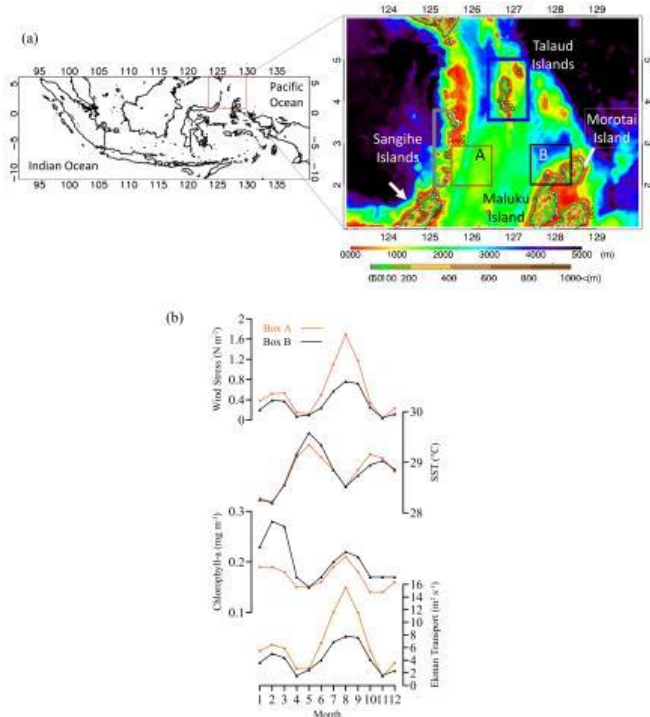


Fig. 1 (a) Topography and bathymetry (m) of the Sangihe-Talaud Islands. (b) Time series of wind stress, SST, chlorophyll-a, and Ekman transport over regions of 125.5°E-126.5°E, 2°N-3°N (Box A) and of 127.5°E-128.5°E, 2°N-3°N (Box B)

2. Materials and Methods

To investigate the wind variability in the region of interest, we analyzed daily gridded reprocessed L3 sea surface winds data of the Advanced Scatterometer (ASCAT) for 2007-2019. The data has a spatial resolution of $0.125^\circ \times 0.125^\circ$, and its accuracy has been tested and validated for coastal and open ocean applications [20]. The wind data is available at the Copernicus Marine Environment Monitoring Service [25].

To decipher the effect of wind variability on the sea surface off the STI, we analyzed Level-3 data of semi-daily 11- μm SST and daily surface chlorophyll-a concentration retrieved from the Moderate Resolution Imaging Spectroradiometer (MODIS). Data have a spatial resolution of $0.04^\circ \times 0.04^\circ$ [21] and were verified against *in situ* measurements [22]. The chlorophyll-a and SST data are archived and distributed by the Physical Oceanography Distributed Active Archive Center (<https://podaac.jpl.nasa.gov/dataaccess>). The analysis period of chlorophyll-a and SST was from January 2007 to October 2019.

We used the Oceanic Niño Index (ONI) to determine ENSO events (El Niño and La Niña) and the Dipole Mode Index (DMI) to define IOD events. Specifically, we used the Niño3.4 SST anomaly index. The ONI data is provided by the National Ocean and Atmospheric Administration Climate Prediction Center and is accessible at <https://www.cpc.ncep.noaa.gov/data/indices/oni.ascii.txt>. The DMI data is generated by the Japanese Agency

for Marine-Earth Science Technology (JAMSTEC) and is attainable at <https://stateoftheocean.osmc.noaa.gov/sur/ind/dmi.php>.

The wind data allow us to calculate wind stress (τ) on the ocean surface and Ekman Mass Transport (EMT) using the formula of [23]:

$$\tau = \rho_a C_d U_{10}^2 \quad (1)$$

$$EMT_x = \frac{(\delta \tau_x + f \tau_y)}{\rho_w (f^2 + \delta^2)} \quad (2a)$$

$$EMT_y = \frac{(\delta \tau_y - f \tau_x)}{\rho_w (f^2 + \delta^2)} \quad (2b)$$

where ρ_a is the air density (1.25 kg m^{-3}), ρ_w is the seawater density ($1.025 \times 10^3 \text{ kg m}^{-3}$), C_D is the drag coefficient, U_{10} is the wind speed 10 m above sea level, δ is frictional dumping parameter (480^{-1} days), and f is the Coriolis parameter. EMT_x and EMT_y denote EMT in zonal and meridional direction, respectively.

All daily and semi-daily data described above were composited into monthly means. The data were then computed into monthly climatological means using the equation of [24]:

$$\bar{X}(x, y) = \frac{1}{n} \sum_{i=1}^n x_i(x, y, t) \quad (3)$$

where $\bar{X}(x, y)$ is monthly mean or monthly climatology value at location (x, y) , $x_i(x, y, t)$ is the i th value of the data at (x, y) , and time t , n is the number of data in one month and the number of monthly data in one period of climatology (2007-2019). If x_i is a hollow pixel, then the pixel is excluded in the calculation.

In order to better understand the temporal variability of surface wind, SST, and surface chlorophyll-a in the ocean region off the STI, we constructed monthly climatology time series for those parameters averaged from 125.5°E-126.5°E; 2°N-3°N (Box A) and 127.5°E-128.5°E; 2°N-3°N (Box B), as depicted in Fig. 1b.

We performed monthly anomaly analysis to all parameters to examine the effects of the 2015 El Niño and the 2019 positive IOD on sea surface conditions off the STI. Furthermore, we correlate all parameters with the ONI and the DMI to highlight the effect of extreme climate events on the study site.

3. Results

Fig. 2a and 3a demonstrate the monthly climatology of ocean surface wind stress over the study area during Northwest Monsoon (January-March) and Southeast Monsoon (July-September), respectively. It is seen that the northeasterly winds prevail from January to March with a magnitude of $4\text{-}5 \times 10^{-1} \text{ N m}^{-2}$. From July to August, southerly wind stress prevails over the STI and its adjacent seas. During this period, the magnitude of wind stress is higher ($> 6 \times 10^{-1} \text{ N m}^{-2}$) than that during Northwest Monsoon, with the strongest wind stress occurring in August.

Fig. 2b and 3b depict monthly climatology of SST during Northwest and Southeast Monsoons. In general, the ocean region off the STI experiences SST cooling

($\sim 28^{\circ}\text{C}$) from January to March. On the other hand, SST off the STI shows relatively higher during Southeast Monsoon than SST during Northwest Monsoon. An SST boundary is observed in this monsoon season, i.e., the ocean region of the eastern Sangihe Islands is dominated by low SST ($<28.5^{\circ}\text{C}$). In contrast, the western side is characterized by warmer SST (30°C).

Fig. 2c and 3c show monthly climatology of surface chlorophyll-a concentration off the STI during Northwest and Southeast Monsoons. There are two different phytoplankton bloom occurrences off the STI throughout the year. The first bloom takes place off the Morotai Island during Northwest Monsoon (denoted by a white arrow in Fig. 2c), whereas the second bloom develops occurs during Southeast Monsoon.

Fig. 2d and 3d illustrate climatological conditions of EMT during Northwest and Southeast Monsoons. In line with surface stress, strong EMT ($> 10 \text{ m}^2 \text{ s}^{-1}$) was observed in the ocean region off the STI during Southeast Monsoon (July-September). In contrast, relatively weak EMT persisted during Northwest Monsoon (January-March). The dominant direction of EMT during Southeast Monsoon (Northwest Monsoon) is eastward (westward).

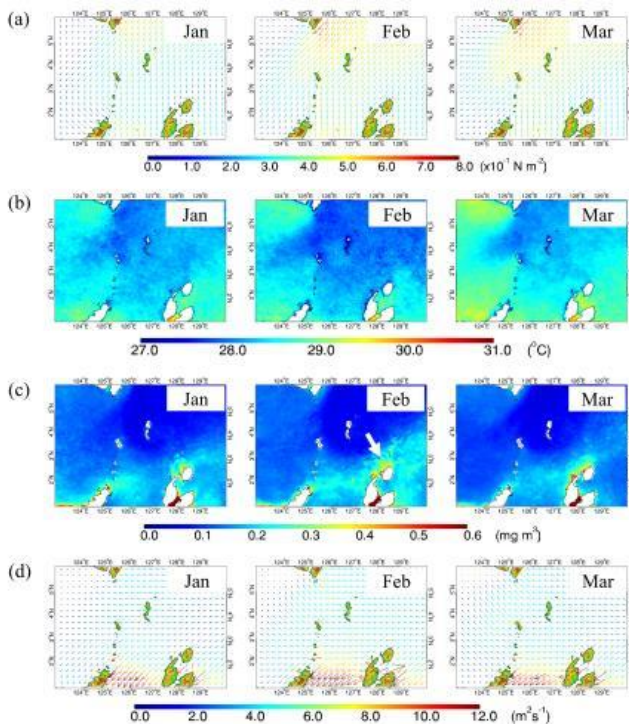


Fig. 2 Monthly climatology maps of (a) surface wind stress, (b) SST, (c) surface chlorophyll-a, and (d) EMT during Northwest Monsoon

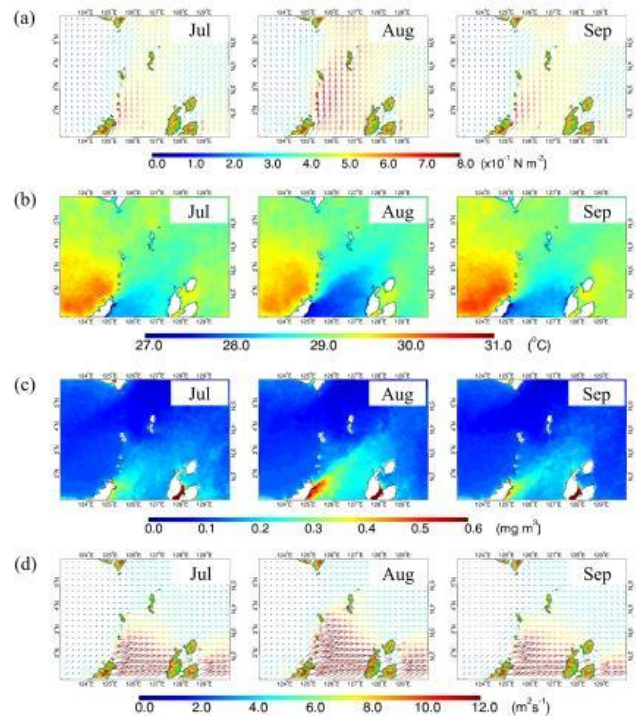


Fig. 3 Monthly climatology maps of (a) surface wind stress, (b) SST, (c) surface chlorophyll-a, and (d) EMT during Southeast Monsoon

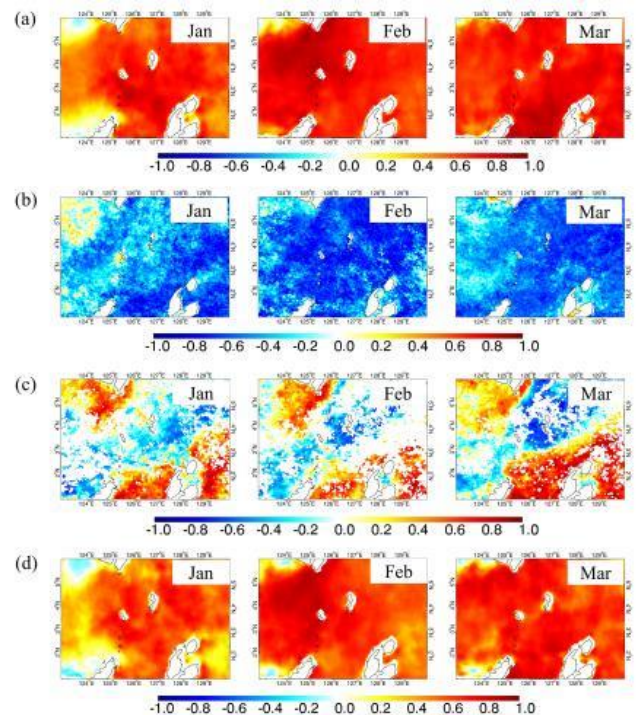


Fig. 4 Correlation between ONI and monthly climatological (a) surface wind stress, (b) SST, (c) surface chlorophyll-a, (d) EMT during Northwest Monsoon

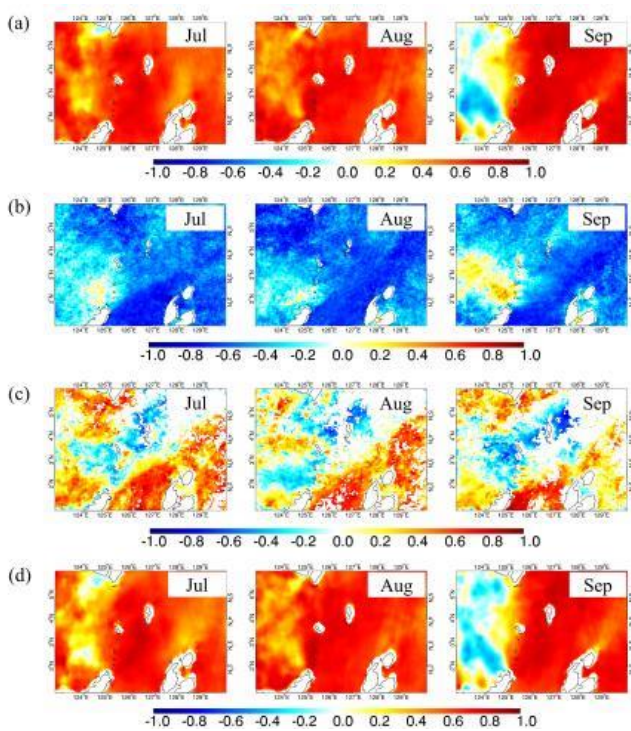


Fig. 5 Correlation between ONI and monthly climatological (a) surface wind stress, (b) SST, (c) surface chlorophyll-a, (d) EMT during Southeast Monsoon

4. Discussion

This research demonstrates that AIM winds strongly influence the variability of sea surface conditions off the STI. During Northwest Monsoon (January-March), the northeasterly winds prevail and may exert stresses on the sea surface of the region of interest, generating mixing in the sea surface and causing SST cooling. We expect the mixing caused elevation in surface chlorophyll-a concentration; however, Fig 2c exhibits low chlorophyll-a concentration. Interestingly, a relatively high chlorophyll-a concentration appeared in the coastal zones of the northern Maluku and Morotai Islands (denoted by white arrows in Fig. 2c). According to the time series of Box B (Fig. 1b), the highest chlorophyll-a concentration (0.28 mg m^{-3}) in the region occurred in February. This concentration might be due to alongshore wind stresses over the northern Maluku and Morotai Islands favorable for subsurface nutrient-rich water's upwelling to the sea surface. Although the signature is not robust, there is a good agreement between chlorophyll-a and EMT (Fig. 1b), i.e., relatively high surface chlorophyll-a concentration corresponds to relatively strong EMT, suggesting the EMT plays a role in increasing chlorophyll-a concentration in that area. It is important to note that upwelling discussed here is the case of northern hemisphere upwelling.

During Southeast Monsoon, the sea surface off the STI shows distinct conditions. Strong southerly wind stresses ($> 5 \times 10^{-1} \text{ N m}^{-2}$) persisted in the region and presumably forced Ekman upwelling, as indicated by cold SST and elevated surface chlorophyll-a

concentration (Fig. 3b and 3c). As a result, sea surfaces off the eastern Sangihe Islands and southern Talaud Islands are supplied with nutrients that can activate phytoplankton bloom. This inference is corroborated by the EMT data that indicate higher EMT values ($> 10 \text{ m}^2 \text{ s}^{-1}$) during Southeast Monsoon compared to EMT values during Northwest Monsoon (Fig. 1b and Fig. 3d). Our results show that the interaction between winds and islands is obvious here. The presence of the northern Sulawesi peninsula (denoted by a white arrow in Fig. 1a) and the Sangihe Islands acts as a barrier for the southerly winds. Strong southerly winds are only observed in the eastern Sangihe Islands and Sulawesi peninsula. The high relief of the northern Sulawesi peninsula likely blocks the wind, producing different wind regime that affects sea surface condition. The sea surface under influencing strong wind stresses shows higher EMT, lower SST, and higher surface chlorophyll-a concentration compared to the sea surface off the western Sangihe Islands and Sulawesi peninsula (Fig. 3). Furthermore, this observation suggests that the variability of sea surface wind determines surface marine productivity in the studied area. It is evident here that the chlorophyll-a maxima diminished when the wind forcing and EMT weakened (Fig. 1b).

The present research also examines the effect of ENSO and IOD on sea surface wind and sea surface conditions off the STI. We found a remarkable positive correlation between ENSO and surface wind stresses during Northwest (Fig. 4a) and Southeast Monsoons (Fig. 5a). A similar pronounced correlation was also observed between ENSO and EMT (Fig. 4d and 5d). Indeed, this observation suggests intense mixing/upwelling occurrences in the region as corroborated by an apparent negative correlation between ENSO and SST (Fig. 4b and 5b). This premise is further supported by the correlation between ENSO and surface chlorophyll-a that suggests the dominant influence of ENSO on the surface marine productivity (Fig. 4c and 5c).

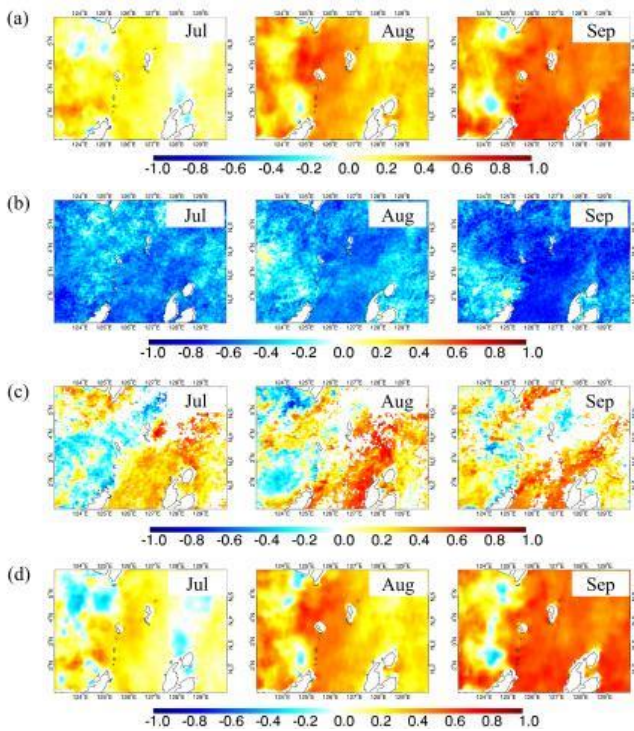


Fig. 6 Correlation between DMI and monthly climatological (a) surface wind stress, (b) SST, (c) surface chlorophyll-a, (d) EMT during Northwest Monsoon

The correlation between IOD and ocean surface parameters during Northwest and Southeast Monsoons is depicted in Fig. 6 and 7, respectively. In comparison to ENSO, the effect of IOD on sea surface condition off the STI during Northwest Monsoon is faint. Negative correlations between IOD and surface wind stress (Fig. 6a) and EMT (Fig. 6d) are noticeable during this monsoon season. Apparently, these wind stresses cannot promote surface mixing/upwelling, as indicated by a positive correlation between IOD and SST (Fig. 6c). We notice a weak positive correlation between IOD and surface chlorophyll-a correlation from February to March (Fig. 6c), suggesting another force influenced surface chlorophyll-a concentration in the region that will be our future study focus. Meanwhile, the influence of IOD on surface winds and EMT is apparent, indicated by positive correlations, during Southeast Monsoon (Fig. 7a and 7d). Congruent with this observation, IOD-SST and IOD chlorophyll-a correlations also show a good agreement, i.e., there is a marked SST cooling (negative correlation; Fig. 7b) and increased surface chlorophyll-a concentration (positive correlation; Fig. 7c), implying the IOD plays a role in determining sea surface condition off the STI during this season.

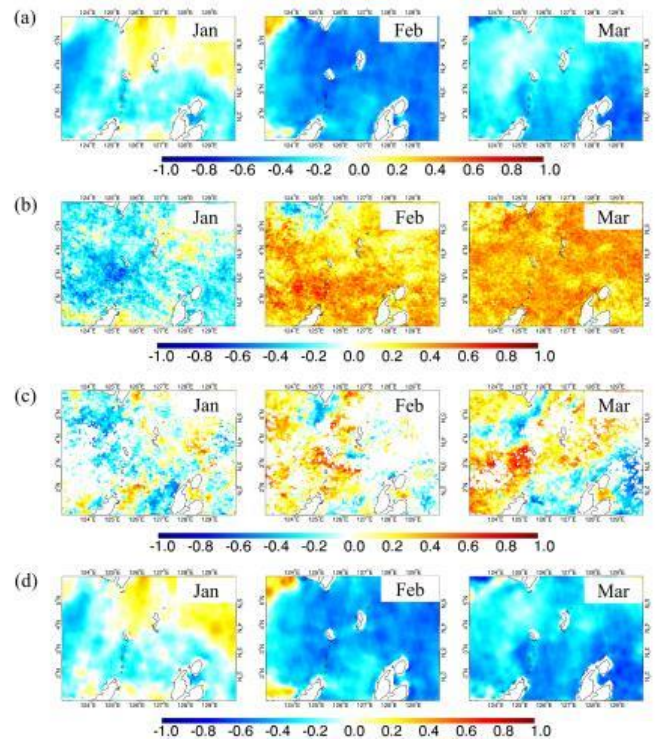


Fig. 7 Correlation between DMI and monthly climatological (a) surface wind stress, (b) SST, (c) surface chlorophyll-a, (d) EMT during Southeast Monsoon

The present research also examines extreme climate events, particularly the 2015 El Niño and the 2019 positive IOD, on sea surface wind intensity over the ocean region off the STI during Southeast Monsoon. We focus on the Southeast Monsoon due to the robust effect of these extreme events being prominent during this monsoon season. When the extreme event took place in 2015, striking positive anomalies can be seen in surface wind stresses (Fig. 8a), surface chlorophyll-a concentration (Fig. 8c), and EMT (Fig. 8d). Fig. 8a shows strong wind stress ($> 0.8 \times 10^{-1} \text{ N m}^{-2}$) and EMT anomalies ($> 5 \text{ m}^2 \text{ s}^{-1}$) dominate the region of interest from July to September. It is visible here that the existence of the northern Sulawesi peninsula shaped the wind regime in the study site. Specifically, the location and direction of strong wind stress and EMT anomalies are well fit with the position of significant negative SST, and positive chlorophyll-a anomalies (Fig. 8b and 8c), suggesting the spatial distribution of sea surface productivity off the STI is primarily controlled by the strength and direction of the wind stresses. During the Southeast Monsoon of 2015, SST and surface chlorophyll-a anomalies attained $< -1^\circ\text{C}$ and 0.5 mg m^{-3} , respectively. Such anomaly may yield a consequence on the regional seafood via decline or increase of fisheries production.

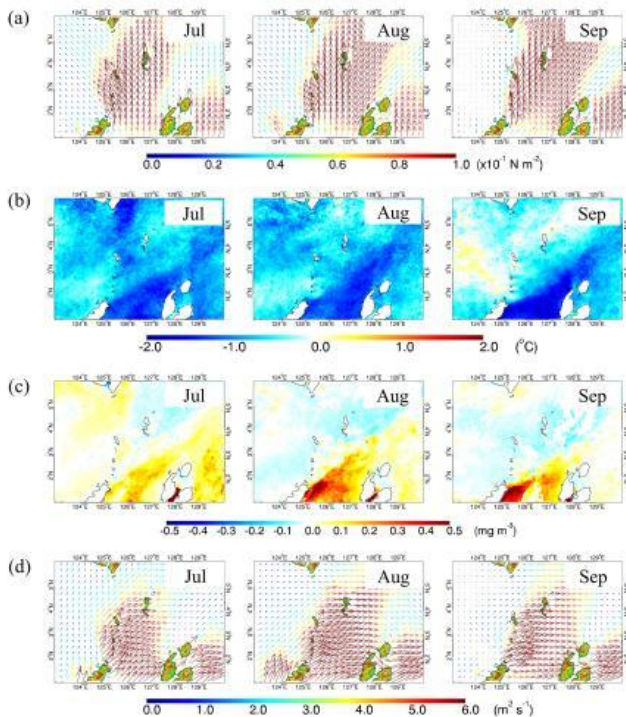


Fig. 8 Anomaly maps of (a) surface wind stress, (b) SST, (c) surface chlorophyll-a, and (d) EMT during Southeast Monsoon of 2015

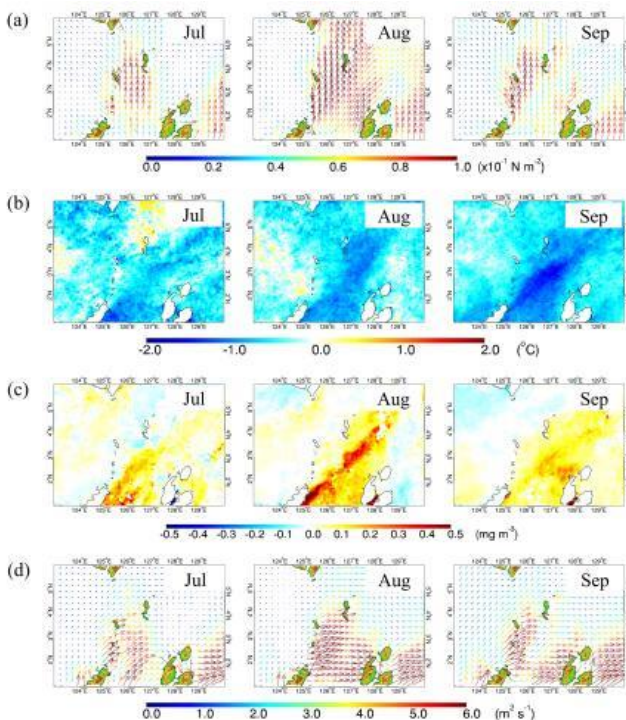


Fig. 9 Anomaly maps of (a) surface wind stress, (b) SST, (c) surface chlorophyll-a, and (d) EMT during Southeast Monsoon of 2019

During the 2019 positive IOD event (July-September), sea surface condition off the STI showed significant positive anomalies in surface wind stress ($> 0.8 \times 10^{-1} \text{ N m}^{-2}$), surface chlorophyll-a concentration ($> 0.2 \text{ mg m}^{-3}$), EMT ($> 5 \text{ m}^2 \text{ s}^{-1}$), and negative SST anomaly (-1°C), as demonstrated by Fig. 9. Again, the center of positive chlorophyll-a anomaly is consistent with wind stress, SST, and EMT anomalies (Fig. 9).

We suggest this positive chlorophyll-a anomaly is possibly due to intense vertical mixing of the mixed layer by robust wind stresses, which leads to cold SST. According to Fig. 8 and 9, we conclude that the effect of the 2015 extreme climate event on the sea surface off the STI is more robust compared to the 2019 extreme climate event. This difference might be due to the proximity of STI to the Pacific Ocean than to the Indian Ocean; hence the region receives the stronger impact of ENSO.

5. Conclusion

Our research has demonstrated that satellite-derived sea surface wind stress, SST, and surface chlorophyll-a concentration are applicable in revealing sea surface variability off the STI. It is important to note that the present research results need to be compared with *in situ* measurement once it is available. Nevertheless, we discovered that both northeasterly and southerly winds play a major role in determining sea surface conditions in the study area, i.e., by lowering SST and enhancing surface chlorophyll-a. The SST cooling and chlorophyll-a maxima occur in response to enhanced monsoonal wind stress and EMT. On the other hand, the SST cooling and chlorophyll-a maxima deteriorated when wind stress and EMT weakened. Furthermore, our correlation analysis revealed that the ENSO plays a dominant role in determining sea surface condition off the STI than the IOD, probably due to its proximity to the Pacific Ocean. Our anomaly analysis also suggests that all anomalies' magnitude and spatial distribution are more robust during the climate extreme events of 2015 compared to 2019. In general, the results of this research highlight the importance of extreme climate events in creating ocean conditions; they can be used for better managing fish resources in the region in the possible future seafood crisis.

References

- [1] SETIAWAN R.Y., SETYOBUDI E., WIRASATRIYA A., MUTTAQIN A.S., and MASLUKAH L. The influence of seasonal and interannual variability on surface chlorophyll-a off the western Lesser Sunda Islands. *IEEE Journal of Selected Topics in Applied Earth Observations and Remote Sensing*, 2019, 12(11): 4191-4197.
- [2] SETIAWAN R.Y., WIRASATRIYA A., HERNAWAN U., LEUNG S., ISKANDAR I. Spatio-temporal variability of surface chlorophyll-a in the Halmahera Sea and its relation to ENSO and the Indian Ocean Dipole. *International Journal of Remote Sensing*, 2020, 41(1): 284-299.
- [3] WIRASATRIYA A., SUGIANTO D.N., MASLUKAH L., AHKAM M.F., WULANDARI S.Y., and HELMI M. Carbon dioxide flux in the Java Sea estimated from satellite measurements. *Remote Sensing Applications: Society and Environment*, 2020, 41(21): 8475-8496.
- [4] WIRASATRIYA A., SUGIANTO D.N., HELMI M., SETIAWAN R.Y., and KOCH M. Distinct characteristics of SST variabilities in the Sulawesi Sea and the northern part of the Maluku Sea during the Southeast Monsoon. *IEEE*

Journal of Selected Topics in Applied Earth Observations and Remote Sensing, 2019, 12(6): 1763-1770.

- [5] SISWANTO E., HORII T., ISKANDAR I., and LUMBAN-GAOL J. Impacts of climate changes on the phytoplankton biomass of the Indonesian Maritime Continent. *Journal of Marine Systems*, 2020, 212: 1-15.
- [6] KURNIAWATI N., SARI Q.W., SETIAWAN R.Y., SISWANTO E., FAUZIYAH, SETIABUDIDAYA D., and ISKANDAR I. Surface chlorophyll-a variations along the southern coast of Java during two contrasting Indian Ocean dipole events: 2015 and 2016. *Journal of Sustainability Science and Management*, 2021, 16(3): 116-127.
- [7] WIRASATRIYA A., SETIAWAN J.D., SUGIANTO D.N., ROSYADI I.A., HARYADI H., WINARSO G., SETIAWAN R.Y., and SUSANTO R.D. Ekman dynamics variability along the southern coast of Java revealed by satellite data. *International Journal of Remote Sensing*, 2020, 41(21): 8475-8496.
- [8] SETIAWAN A., SUPRIYADI F., NOOR G.E., FADLI M, and MUDRIMANTO A. *The marine and fisheries profile of the Sangihe Islands Regency and Talaud Islands Regency, North Sulawesi Province (in Indonesian)*. Jakarta, Indonesia: Ministry of Marine Affairs and Fisheries of the Republic of Indonesia, 2016.
- [9] FENG M., ZHANG N., LIU Q., and WIJFFELS S. The Indonesian throughflow, its variability and centennial change. *Geoscience Letters*, 2018, 5(3): 1-10.
- [10] WIJAYANTI L.A.S., FITRIYA N., FIRDAUS M.R., SATRIYO T. B., DJUMANTO, SETIAWAN R. Y., NURDIN N., HELMI M., and ZAINUDDIN M. Deep-sea phytoplankton community of the Sangihe-Talaud Islands waters. *Aquaculture, Aquarium, Conservation & Legislation Bioflux*, 2020, 13(5): 3212-3223.
- [11] CHRISTIE P., PIETRI D.M., STEVENSON T.C., POLLNAC R., KNIGHT M., and WHITE A.T. Improving human and environmental conditions through the Coral Triangle Initiative: progress and challenges. *Current Opinion in Environmental Sustainability*, 2016, 19: 169-181.
- [12] YUN K.S., LEE J.Y., TIMMERMANN A., STEIN K., STUECKER M.F., FYFE J.C., and CHUNG E.-S. Increasing ENSO-rainfall variability due to changes in future tropical temperature-rainfall relationship. *Communications Earth & Environment*, 2021, 2(43): 1-7.
- [13] CAI W., WANG G., GAN B., WU L., SANTOSO A., LIN X., CHEN Z., JIA F., and YAMAGATA T. Stabilised frequency of extreme positive Indian Ocean Dipole under 1.5 °C warming. *Nature Communication*, 2018, 9(1419): 1-8.
- [14] PALMEIRO F.M., IZA M., BARRIOPEDRO D., CALVO N., and GARCÍA-HERRERA R. The complex behavior of El Niño winter 2015–2016. *Geophysical Research Letters*, 2017, 44: 2902-2910.
- [15] HU S. and FEDOROV A.V. The extreme El Niño of 2015–2016 and the end of global warming hiatus. *Geophysical Research Letters*, 2017, 44: 3816-3824.
- [16] L'HEUREUX M.L., TAKAHASHI K., WATKINS A.B., BARNSTON A.G., BECKER E.J., DI LIBERTO T.E., GAMBLE F., GOTTSCHALCK J., HALPERT M.S., HUANG B., MOSQUERA-VÁSQUEZ K., and WITTENBERG A.T. Observing and predicting the 2015-16 El Niño. *Bulletin of the American Meteorological Society*, 2016, 98 (7): 1363-1382.
- [17] LEVINE A.F.Z. and MCPHADEN M.J. How the July 2014 easterly wind burst gave the 2015-2016 El Niño a head

start. *Geophysical Research Letters*, 2016, 43: 6503-6510.

- [18] LU B. REN H-L. What Caused the Extreme Indian Ocean Dipole Event in 2019? *Geophysical Research Letters*, 2020, 47(11).
- [19] DELMAN A.S., SPRINTALL J.J., MCCLEAN L., and TALLEY L.D. Anomalous Java cooling at the initiation of positive Indian Ocean Dipole events. *Journal of Geophysical Research: Oceans*, 2016, 121: 5805-5824.
- [20] LINDSLEY R.D., BLODGETT J.R., and LONG D.G. Analysis and validation of high-resolution wind from ASCAT. *IEEE Transactions on Geoscience and Remote Sensing*, 2016, 54 (10): 5699-5711.
- [21] UMBERT M., GUIMBARD S., POY. J. B., and TURIEL A. Synergy between ocean variables: remotely sensed surface temperature and chlorophyll concentration coherence. *Remote Sensing*, 2020, 12(7): 1-13.
- [22] GHANEA M., MORADI M., KABIRI K., and MEHDINIA A. Investigation and validation of MODIS SST in the northern Persian Gulf. *Advances in Space Research*, 2016, 57(1): 127-136.
- [23] WIRASATRIYA A., SUSANTO R.D., KUNARSO K., JALIL A.R., RAMDANI F., and PURYAJATI A.D. Northwest monsoon upwelling within the Indonesian seas. *International Journal of Remote Sensing*, 2021, 42(14): 5433-5454.
- [24] WIRASATRIYA A., SETIAWAN R.Y., and SUBARDJO P. The effect of ENSO on the variability of chlorophyll-a and sea surface temperature in the Maluku Sea. *IEEE Journal of Selected Topics in Applied Earth Observations and Remote Sensing*, 2017, 10(12): 5513-5518.
- [25] COPERNICUS MARINE SERVICE, n.d. <https://marine.copernicus.eu/>

参考文献:

- [1] SETIAWAN R.Y., SETYOBUDI E., WIRASATRIYA A., MUTTAQIN A.S. 和 MASLUKAH L. 季節性和年際變化對小巽他群島西部表面葉綠素 a 的影響。電氣和電子工程師學會應用地球觀測與遙感選題雜誌, 2019, 12(11): 4191-4197。
- [2] SETIAWAN R.Y.、WIRASATRIYA A.、HERNAWAN U.、LEUNG S.、ISKANDAR I. 哈馬黑拉海表面葉綠素一種的時空變異性及其與厄爾尼諾-南方濤動和印度洋偶極子的關係。國際遙感雜誌, 2020, 41(1): 284-299。
- [3] WIRASATRIYA A.、SUGIANTO D.N.、MASLUKAH L.、AHKAM M.F.、WULANDARI S.Y. 和 HELMI M. 根據衛星測量估算的爪哇海二氧化碳通量。遙感應：社會與環境, 2020, 41(21) : 8475-8496。
- [4] WIRASATRIYA A.、SUGIANTO D.N.、HELMİ M.、SETIAWAN R.Y. 和 KOCH M. 東南季風期間蘇拉威西海和馬魯古海北部海溫變化的不同特徵。電氣和電子工程師學會 應用地球觀測和遙感選定主題雜誌。2019, 12 (6) : 1763-1770。

- [5] SISWANTO E.、HORII T.、ISKANDAR I. 和 LUMBAN-GAOL J. 氣候變化對印度尼西亞海洋大陸浮游植物生物量的影響。海洋系統雜誌, 2020 年, 212 : 1-15。
- [6] KURNIAWATI N.、SARI Q.W.、SETIAWAN R.Y.、SISWANTO E.、FAUZIYAH SETIABUDIDAYA D., 和 ISKANDAR I. 兩個對比鮮明的印度洋偶極子事件期間爪哇南部海岸的表面葉綠素-a 變化: 2015 年和 2016 年。可持續發展科學與管理雜誌, 2021 年, 16(3) : 116-127。
- [7] WIRASATRIYA A.、SETIAWAN J.D.、SUGIANTO D.N.、ROSYADI I.A.、HARYADI H.、WINARSO G.、SETIAWAN R.Y. 和 SUSANTO R.D. 埃克曼沿爪哇南部海岸的動態變化由衛星數據顯示。國際遙感雜誌, 2020 , 41(21) : 8475-8496。
- [8] SETIAWAN A.、SUPRIYADI F.、NOOR G.E.、FADLI M 和 MUDRIMANTO A. 北蘇拉威西省桑吉赫群島攝政和塔勞德群島攝政的海洋和漁業概況 (印度尼西亞)。印度尼西亞雅加達: 印度尼西亞共和國海洋事務和漁業部, 2016 年。
- [9] FENG M., ZHANG N., LIU Q., 和 WIJFFELS S. 印度尼西亞的通流、它的變異性和百年變化。地球科學快報, 2018, 5(3): 1-10。
- [10] WIJAYANTI L.A.S.、FITRIYA N.、FIRDAUS M.R.、SATRIYO T. B.、DJUMANTO、SETIAWAN R. Y.、NURDIN N.、HELMY M. 和 ZAINUDDIN M. 桑吉赫-塔勞群島的深海浮游植物群落水產養殖、水族館、保護與立法生物通量, 2020, 13(5): 3212-3223。
- [11] CHRISTIE P.、PIETRI D.M.、STEVENSON T.C.、POLLNAC R.、KNIGHT M. 和 WHITE A.T. 通過珊瑚三角倡議改善人類和環境條件: 進步和挑戰。環境可持續性現狀, 2016, 19 : 169-181。
- [12] YUN K.S.、LEE J.Y.、TIMMERMANN A.、STEIN K.、STUECKER M.F.、FYFE J.C. 和 CHUNG E.-S. 由於未來熱帶溫度 - 降雨量關係的變化, 增加了厄爾尼諾-南方濤動- 降雨量的變異性。通信地球與環境, 2021 年, 2(43) : 1-7。
- [13] CAI W., WANG G., GAN B., WU L., SANTOSO A., LIN X., CHEN Z., JIA F., 和 YAMAGATA T. 1.5° 下極端正印度洋偶極子的穩定頻率 C. 升溫。自然通訊, 2018, 9(1419): 1-8。
- [14] PALMEIRO F.M.、IZA M.、BARRIOPEDRO D.、CALVO N. 和 GARCÍA-HERRERA R. 厄爾尼諾冬季 2015-2016 的複雜行為。地球物理研究快報, 2017, 44 : 2902-2910。
- [15] HU S. 和 FEDOROV A.V. 2015-2016 年的極端厄爾尼諾現象和全球變暖中斷的結束。地球物理研究快報, 2017, 44 : 3816-3824。
- [16] L'HEUREUX M.L., TAKAHASHI K., WATKINS A.B., BARNSTON A.G., BECKER E.J., DI LIBERTO T.E., GAMBLE F., GOTTSCHALCK J., HALPERT M.S., HUANG B., MOSQUERA-VÁSQUEZ K., 和 WITTENBERG A.T. 觀測和預測 2015-16 年厄爾尼諾現象。美國氣象學會公報, 2016, 98 (7) : 1363-1382。
- [17] LEVINE A.F.Z. 和 MCPHADEN M.J. 2014 年 7 月的東風爆發如何讓 2015-2016 年的厄爾尼諾現象領先一步。地球物理研究快報, 2016, 43 : 6503-6510。
- [18] 盧伯. 任海倫. 是什麼導致了 2019 年極端印度洋偶極子事件? 地球物理研究快報, 2020, 47(11)。
- [19] DELMAN A.S.、SPRINTALL J.J.、MCCLEAN L. 和 TALLEY L.D. 正印度洋偶極子事件開始時爪哇異常冷卻。地球物理研究雜誌: 海洋, 2016, 121 : 5805-5824。
- [20] LINDSLEY R.D.、BLODGETT J.R. 和 LONG D.G. 來自高級散射計的高分辨率風的分析和驗證。電氣和電子工程師學會地球科學與遙感學報, 2016, 54 (10): 5699-5711。
- [21] UMBERT M., GUIMBARD S., POY. J. B. 和 TURIEL A. 海洋變量之間的協同作用: 遙感表面溫度和葉綠素濃度一致性。遙感, 2020, 12(7): 1-13。
- [22] GHANEA M.、MORADI M.、KABIRI K. 和 MEHDINIA A. 波斯灣北部莫迪斯海面溫度的調查和驗證。空間研究進展, 2016, 57(1): 127-136。
- [23] WIRASATRIYA A.、SUSANTO R.D.、KUNARSO K.、JALIL A.R.、RAMDANI F. 和 PURYAJATI A.D. 印度尼西亞海域上湧的西北季風。國際遙感雜誌, 2021, 42(14): 5433-5454。
- [24] WIRASATRIYA A.、SETIAWAN R.Y. 和 SUBARDJO P. 厄爾尼諾-南方濤動對馬魯古海葉綠素一種和海面溫度變異性的影響。電氣和電子工程師學會應用地球觀測與遙感選題雜誌, 2017, 10(12): 5513-5518。
- [25] 哥白尼海事服務, 未注明日期 <https://marine.copernicus.eu/>